

## Vibrational resonance in neuron populations

Bin Deng, Jiang Wang, Xile Wei, K. M. Tsang, and W. L. Chan

Citation: *Chaos* **20**, 013113 (2010); doi: 10.1063/1.3324700

View online: <http://dx.doi.org/10.1063/1.3324700>

View Table of Contents: <http://chaos.aip.org/resource/1/CHAOEH/v20/i1>

Published by the [American Institute of Physics](#).

---

### Related Articles

Multiscale characterization of recurrence-based phase space networks constructed from time series  
*Chaos* **22**, 013107 (2012)

Optimal pinning synchronization on directed complex network  
*Chaos* **21**, 043131 (2011)

Variability of contact process in complex networks  
*Chaos* **21**, 043130 (2011)

Detecting the topologies of complex networks with stochastic perturbations  
*Chaos* **21**, 043129 (2011)

Vibrational resonance in excitable neuronal systems  
*Chaos* **21**, 043101 (2011)

---

### Additional information on Chaos

Journal Homepage: <http://chaos.aip.org/>

Journal Information: [http://chaos.aip.org/about/about\\_the\\_journal](http://chaos.aip.org/about/about_the_journal)

Top downloads: [http://chaos.aip.org/features/most\\_downloaded](http://chaos.aip.org/features/most_downloaded)

Information for Authors: <http://chaos.aip.org/authors>

### ADVERTISEMENT



*Submit Now*

**Explore AIP's new  
open-access journal**

- **Article-level metrics  
now available**
- **Join the conversation!  
Rate & comment on articles**

# Vibrational resonance in neuron populations

Bin Deng,<sup>1</sup> Jiang Wang,<sup>1</sup> Xile Wei,<sup>1</sup> K. M. Tsang,<sup>2</sup> and W. L. Chan<sup>2</sup>

<sup>1</sup>*School of Electrical and Automation Engineering, Tianjin University, Tianjin 300072, China*

<sup>2</sup>*Department of Electrical Engineering, The Hong Kong Polytechnic University, Kowloon, Hong Kong*

(Received 26 August 2009; accepted 26 January 2010; published online 9 March 2010)

In this paper different topologies of populations of FitzHugh–Nagumo neurons have been introduced to investigate the effect of high-frequency driving on the response of neuron populations to a subthreshold low-frequency signal. We show that optimal amplitude of high-frequency driving enhances the response of neuron populations to a subthreshold low-frequency input and the optimal amplitude dependences on the connection among the neurons. By analyzing several kinds of topology (i.e., random and small world) different behaviors have been observed. Several topologies behave in an optimal way with respect to the range of low-frequency amplitude leading to an improvement in the stimulus response coherence, while others with respect to the maximum values of the performance index. However, the best results in terms of both the suitable amplitude of high-frequency driving and high stimulus response coherence have been obtained when the neurons have been connected in a small-world topology. © 2010 American Institute of Physics.

[doi:10.1063/1.3324700]

**In bistable systems, it has been shown that the role of noise in improving the quality of signal detection can be played by other types of driving, such as a chaotic signal or a high-frequency periodic force. In the latter case, known as *vibrational resonance* (VR), the system is under the action of a two frequency signal. Such bichromatic signals are pervasive in different fields, including brain dynamics, where, for instance, bursting neurons may exhibit two widely different time scales, and telecommunications, where information carriers are usually high-frequency waves modulated by a low-frequency signal that encodes the data. The dynamics of neurons is often modeled by using differential models. Networks of many neurons can be studied by connecting many of these models and studying the global behavior of the system. The importance of these studies is related to a deep understanding of the neural mechanisms underlying neural systems. This paper focuses on several topological structures of networks of these models and studies the dynamical response of coupled neurons to bichromatic signal with two very different frequencies from the viewpoint of VR.**

## I. INTRODUCTION

The external influence can considerably affect the signal detection by nonlinear system. Stochastic resonance (SR), where the response of a nonlinear system to a weak deterministic signal is enhanced by external random fluctuation,<sup>1–3</sup> is the most relevant example of this fact. Recently, Ullner *et al.* gave a detailed description of several new noise-induced phenomena in the FitzHugh–Nagumo (FHN) neuron in Ref. 4. They have investigated the Canard-enhanced SR,<sup>5</sup> the effect of noise-induced signal processing in systems with complex attractors,<sup>6</sup> and a new noise-induced phase transition from a self-sustained oscillatory regime to an excitable behavior.<sup>7</sup> They also showed that optimal amplitude of high-frequency driving enhances the response of

an excitable system to a low-frequency subthreshold signal.<sup>8</sup> In the latter case, known as VR, the system is under the action of two frequency signal.<sup>9–11</sup> Such bichromatic signals are pervasive in many different fields, including brain dynamics,<sup>12</sup> where, for instance, bursting neurons may exhibit two widely different time scales.

However, most of the relevant studies only considered the single neuron.<sup>5,7,8</sup> Recently, Ref. 13 has investigated SR on excitable small-world networks so the focus of this paper is on the investigation of the role of topology in neuron networks in the presence of high-frequency driving. We will refer to the enhancement in the stimulus response due to the presence of high-frequency driving as a generalized VR effect. Several network topologies have been investigated focusing on the positive effects of connections in networks of nonlinear FHN neurons affected by high-frequency driving. Structures, such as chains or fully connected graphs, random graphs, and small-world networks,<sup>14</sup> have been simulated by connecting FHN neurons excited by subthreshold low-frequency signal. The Fourier coefficients have been evaluated to point out the VR features of extended neuron populations versus the topology configuration. The phenomenon studied in this paper is also related to noise-enhanced SR in coupled oscillation.<sup>15,16</sup>

The contents of this paper are arranged as follows. In Sec. II, VR in single FHN neuron is introduced briefly. The analysis of the VR in different models of neuron population is given in Sec. III. Finally, conclusions and discussions are made in Sec. IV.

## II. VIBRATIONAL RESONANCE IN SINGLE FHN MODEL

In the presence of two harmonic signals, the FHN model<sup>17</sup> is defined by the equations

$$\varepsilon \frac{dx}{dt} = x - \frac{x^3}{3} - y, \quad (1)$$

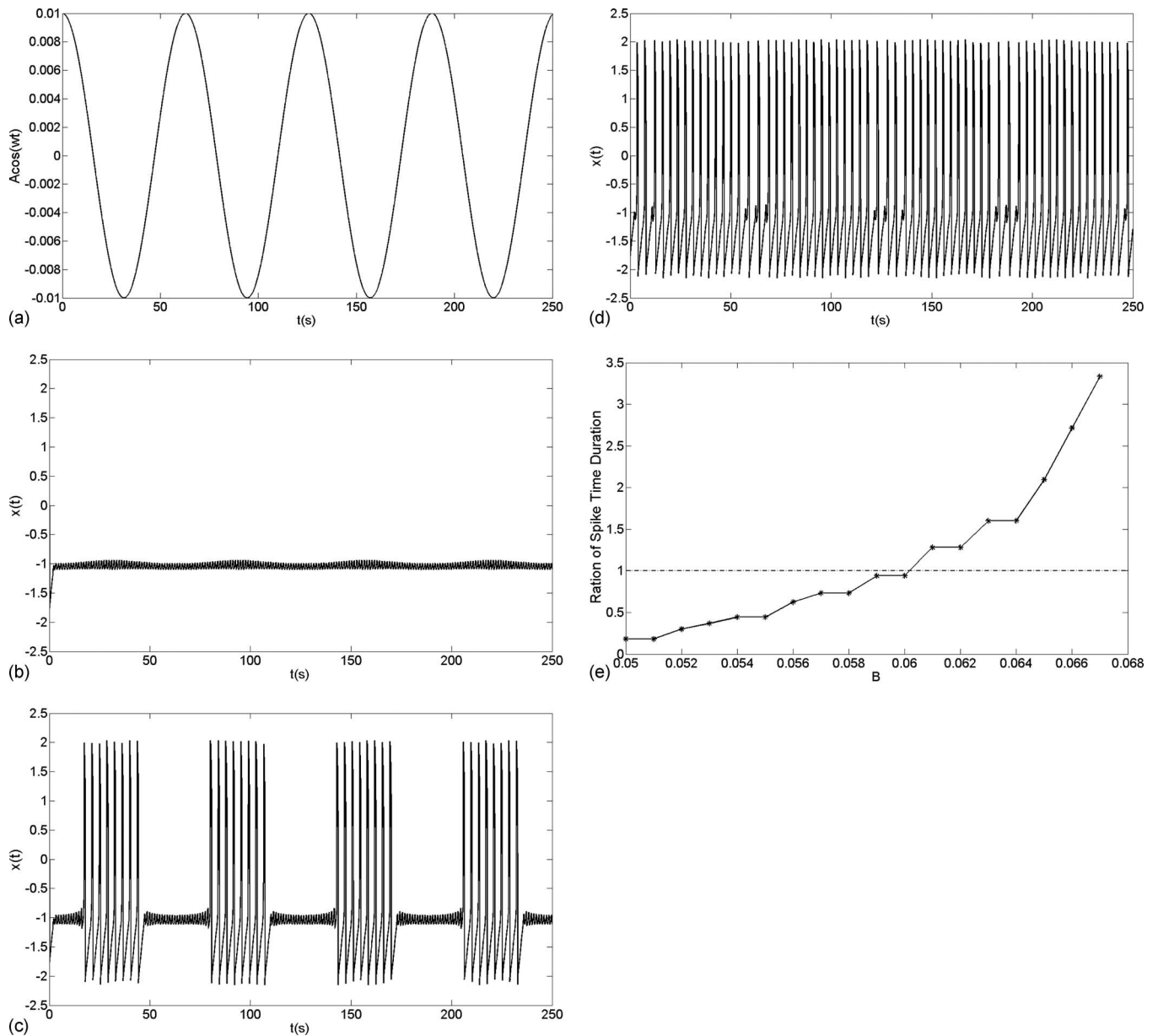


FIG. 1. Firing of a single FHN neuron subjected to a subthreshold low-frequency signal for increasing the amplitude of high-frequency driving: (a) subthreshold low-frequency signal; (b)  $x(t)$  for weak high-frequency driving (no spikes are emitted); (c)  $x(t)$  for optimal high-frequency driving; (d)  $x(t)$  for too strong high-frequency driving. (e) The ratio of the time duration of spikes and subthreshold oscillation vs the amplitude of high-frequency driving.

$$\frac{dy}{dt} = x + a + A \cos(\omega t) + B \cos(\Omega t), \quad (2)$$

where  $x(t)$  represents the membrane potential of neuron and  $y(t)$  is related to the conductivity of the potassium channels existing in the neuron membrane. The value of the time scale ratio  $\varepsilon=0.01$  is chosen so that the activator  $x(t)$  evolves much faster than the inhibitor  $y(t)$ . The terms  $A \cos(\omega t)$  and  $B \cos(\Omega t)$  stand for the low- and high-frequency components of the external signal, respectively. In what follows we will choose  $A=0.01$ , so that the system is below the excitation threshold, and  $\Omega \gg \omega$ , in particular,  $\Omega=5$  and  $\omega=0.1$ . In Eq. (2) we have considered no phase shift between the two driving signals, but it can be checked that the existence of an arbitrary phase shift does not alter the results that follow. The parameter  $a$  determines the behavior of the system. For  $a$

$> 1.0$  the FHN model is excitable, and for  $a < 1.0$  it shows an oscillatory behavior. At the bifurcation  $a=1.0$  the stability of the only fix point will be changed.<sup>18</sup> Between these two cases an intermediate behavior can appear. For values of the parameter  $a$  slightly beyond the bifurcation point, small oscillations near the unstable fix point exist instead of large spike and these are the so-called canard oscillations.<sup>19</sup> An important fact of the treatment of canard oscillation is that a very small change in the parameter  $a$  leads to a large different in the trajectories. This change in the parameter  $a$  can be caused by some instantaneous influence of noise as investigated in Refs. 5 and 18 or external high-frequency driving as investigated in Ref. 8. In this paper, the parameter of  $a$  is fixed to be 1.05. We fix the amplitude of the low-frequency signal component and increase the high-frequency amplitude. In

Fig. 1 the behavior of the system with respect to increasing the amplitude of high-frequency driving is reported. The input is a periodic, underthreshold signal, as shown in Fig. 1(a). As can be noticed when the amplitude of high-frequency driving is low [Fig. 1(b)], the FHN neuron does not fire, but when the amplitude is too high [Fig. 1(d)], the firing is not coherence with the input. The optimal case is represented by Fig. 1(c). As the information is carried through neuron spikes, for a sinusoidal input signal, the more the ratio of the time duration of spikes and subthreshold oscillation is close to 1, the better the information is carried through spike trains. From Fig. 1(e), it can be seen that while the amplitude of high-frequency driving is about 0.06, the information will be carried best.

To evaluate the amplitude of the input frequency in the output signal, we calculate the Fourier coefficient  $Q$  for the input frequency  $\omega$ . We use the  $Q$  parameter instead of the power spectrum because we are interested in the transport of the information encoded in the frequency  $\omega$ . For this task the  $Q$  parameter is a much more compact tool than the power spectrum<sup>1,20</sup>

$$Q_{\sin} = \frac{\omega}{2n\pi} \int_0^{2\pi n/\omega} 2x(t) \sin(\omega t) dt,$$

$$Q_{\cos} = \frac{\omega}{2n\pi} \int_0^{2\pi n/\omega} 2x(t) \cos(\omega t) dt,$$

$$Q = \sqrt{Q_{\sin}^2 + Q_{\cos}^2},$$

where  $n$  is the number of period  $2\pi/\omega$  covered by the integration time. The maximum of  $Q$  shows the best phase synchronization between input signal and output firing. It is to be noted that in the case of phase synchronization one could expect a response of the  $Q$  measure but not vice versa, and the phase synchronization between the input signal and the output of neuron can be seen from the following figures of time series. Also, as information in neuron system is carried through large spikes instead of subthreshold oscillations, we are more interested in the frequency of spikes. So following Ref. 6, we set the threshold  $V_s=0$  in the calculation of  $Q$ . If  $V < V_s$ ,  $V$  is replaced by the value of the fixed point  $V_f$  (here  $V_f=-1$ ); otherwise,  $V$  remains the same.

Figure 2 shows VR in the single FHN neuron with value of parameter  $a=1.05$ . The dependence of neuron's response on the amplitude of the high-frequency driving displays a resonant form with clearly defined maxima at the optimal values of  $B$ , similar to what happens in SR. The staircase form of this dependence is caused by the abrupt discrete appearance of new spikes in the spike train as the forcing amplitude changes.

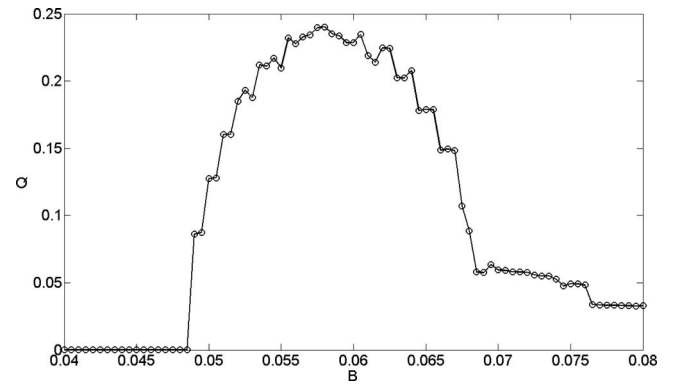


FIG. 2. Response  $Q$  of the FHN neuron at the low frequency  $\omega$  vs the amplitude  $B$  of the high-frequency input signal.

### III. VIBRATIONAL RESONANCE IN NEURON POPULATIONS

Now we consider the coupled FHN neuron populations subject to series of high-frequency driving with the common amplitude and frequency but different phases described by

$$\varepsilon \frac{dx_i}{dt} = x_i - \frac{x_i^3}{3} - y_i - I_i^{\text{syn}}, \quad (3)$$

$$\frac{dy_i}{dt} = x_i + a + A_i \cos(\omega t) + B \cos(\Omega t + \varphi_i), \quad (4)$$

where  $i=1, 2, \dots, N$  index of the neurons. Without loss of generality, let  $\varphi_i$  be uniformly distributed in  $[0, \pi]$ .  $\varepsilon=0.01$ ,  $A_i=0.01$ ,  $\omega=0.1$  and  $\Omega=5$  as used in Sec. II.  $A_i \cos(\omega t)$  and  $B \cos(\Omega t + \varphi_i)$  are low- and high-frequency driving, respectively.  $I_i^{\text{syn}}$  is the synaptic current through neuron  $i$ .

For the electrical coupling,

$$I_i^{\text{syn}} = \sum_{j=i-r}^{j=i+r} g_{\text{syn}} (x_i - x_j), \quad (5)$$

where  $g_{\text{syn}}$  is the conductance of synaptic channel.  $g_{\text{syn}}=0.01$ , which is large enough to synchronize the coupled neurons.  $r$  is the radius of the neighborhood and the value of it will be given in each case followed. By varying  $r$  the network architecture changes from local connection to all-to-all global coupling.

In neural systems with a large amount of neurons, it is unnecessary and impossible to add external signals to all involved individuals. Only weak and local input is reasonable and guarantees the low energy consumption in large neural networks, so in all cases in this paper, the same low-frequency signal has been applied to a fraction  $f$  ( $0 < f < 1$ ) of elements in the neuron populations, whereas high-frequency driving with different phases for each neuron has been taken into account. The response of the entire network has been monitored by considering the average of each membrane variable  $x_i$ , namely,  $V(t) = (1/N) \sum x_i(t)$ .



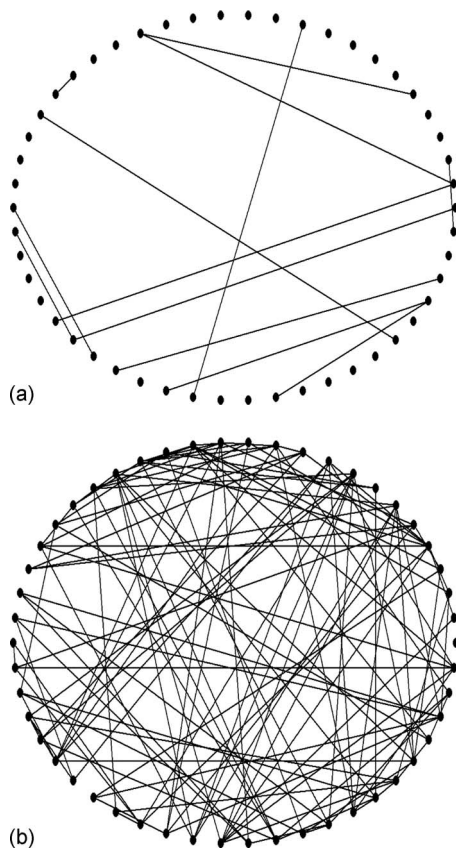


FIG. 3. Example of considered random network topologies. Given 50 isolated nodes, one connects every pair of nodes with probability (a) 0.01, (b) 0.1.

### A. Random connections

First of all, the case in which the neurons are random coupled has been investigated. The random networks are characterized by asymmetric structures and capture in an idealized way the features of many real systems. These networks have a short average path length which drives from the fact that, starting from each node, any other node of the network can be reached in a small number of links.<sup>14</sup> Starting from a population of  $N$  FHN neurons the random network has been built by using the following rule. Given a probability  $p$  of connections, each pair of neurons is connected by a link with probability  $p$  so the topology structure of a random network is determined by the probability, as shown in Fig. 3.

First, we fix  $f=50\%$  and  $p=0.5$  which means that half of the neurons are subjected to the low-frequency signal and each pair of neurons is connected by a link with probability 0.5. The effects of high-frequency driving in a random network of FHN have been characterized with respect to different values of the number of FHN units. The result is shown in Fig. 4(a), where it is evident that increasing the number of FHN units, the response dependence is shifted to the right. The larger the neuron population is, the more energy is needed for the emergence of VR in a randomly coupled neuron network, and while the neuron population is large enough the corresponding high-frequency driving amplitude  $B_{VR}$  of VR will not increase notably with the size of the neuron network, as shown in Fig. 4(b).

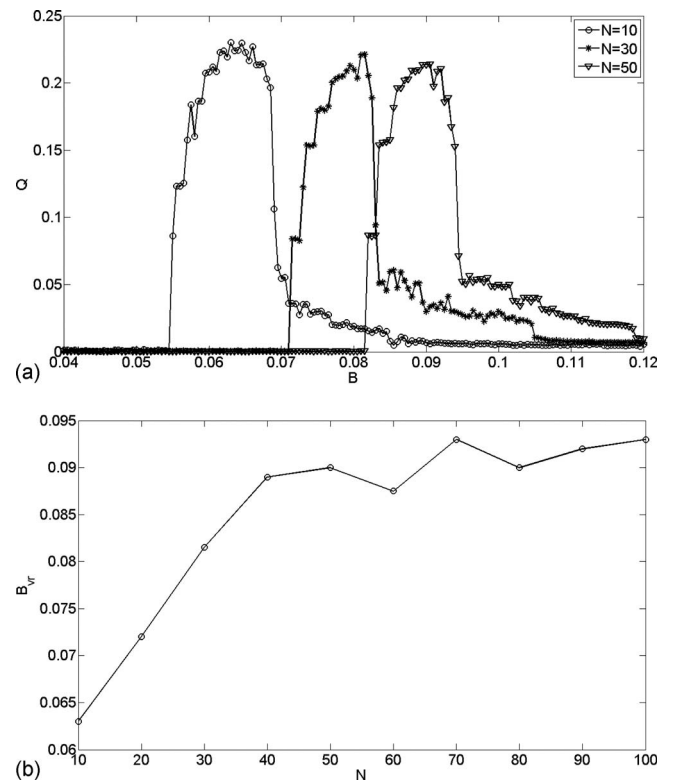


FIG. 4. Effect of the size of neuron network on the VR in a randomly coupled neuron network. (a) Response  $Q$  of three randomly coupled neuron networks with different amounts of elements vs the amplitude  $B$  of high-frequency driving. (b) The corresponding high-frequency driving amplitude  $B_{VR}$  vs the amount of neuron population. The parameters are  $p=0.5$ ,  $f=50\%$ . This figure is the average result of ten trials.

For an Erdős–Rényi (Ref. 21) random graph with  $N$  nodes, if the connection probability  $p$  is greater than a certain threshold  $p_t \sim (\ln N)/N$ , then almost every random graph is connected, so for a randomly coupled neuron network with 50 FHN units, if connection probability is less than  $\ln(50)/50 \approx 0.08$ , there may be some isolated neurons in the network and the value of  $Q$  increases with the increase in  $p$ , as shown in Fig. 5(a). If  $p$  is greater than 0.08, almost every graph is connected, so the value of  $Q$  will not increase with the increase in  $p$ , as shown in Fig. 5(b). If  $p$  is greater than 0.08, the optimal amplitude of high-frequency driving  $B_{VR}$  will increase with the increase in  $p$ , as shown in Fig. 5(d). We suspect that it may be because that while almost every random graph is connected the additional links will lead to more energy cost needed for VR in a randomly coupled neuron population. If  $p$  is less than 0.08,  $B_{VR}$  will not increase with the increase in  $p$ , as shown in Fig. 5(c).

### B. Small-world networks

Many real networks have a short average path length, but at the same time show a high clustering degree due to the presence of both short-range and long-range links. In order to model these systems Strogatz and Watts introduced the concept of small-world networks that successfully captures the essential features of the neuronal systems of the *C. elegans*.<sup>14</sup> Small-world networks can be built starting from a network of locally coupled neurons, i.e., each neuron is

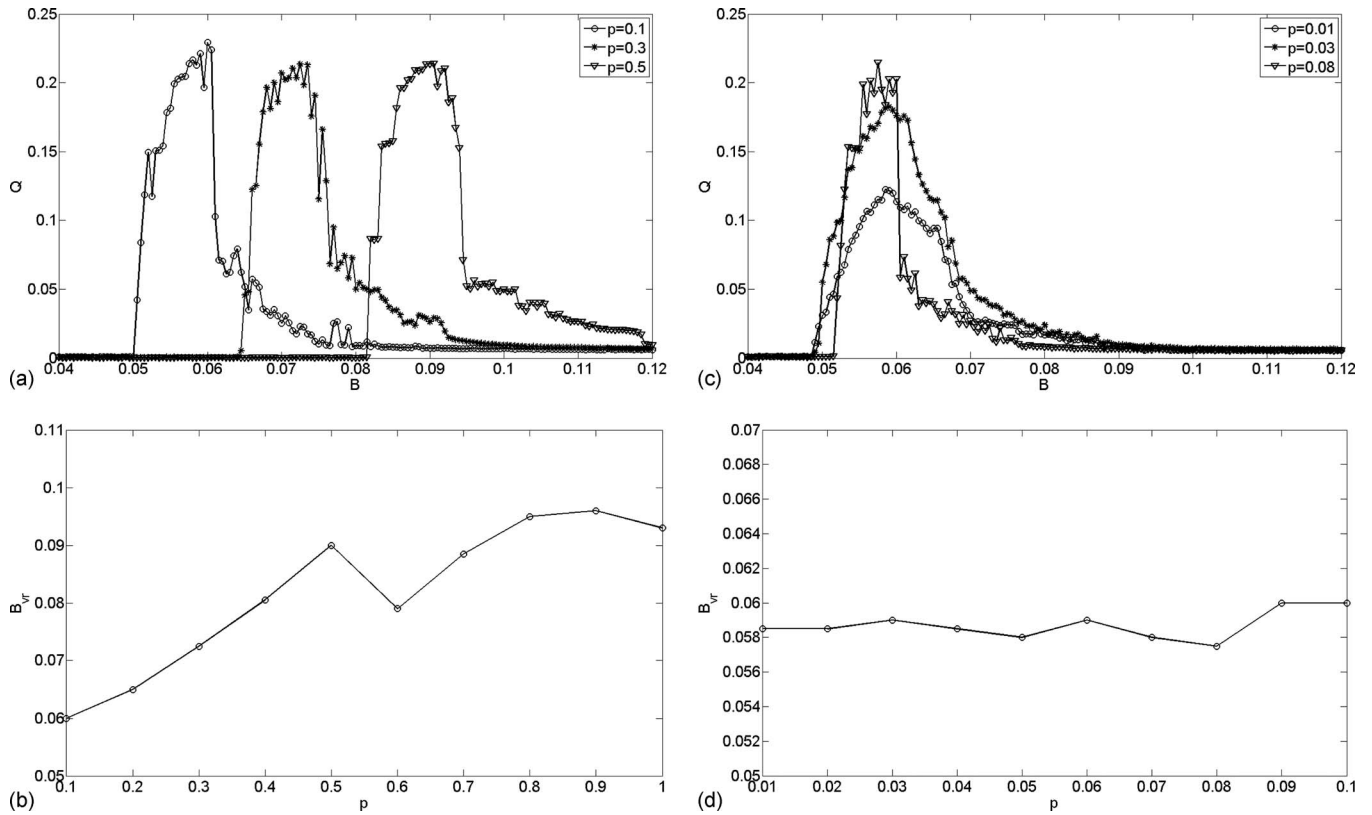


FIG. 5. Effect of the probability of connections on the VR in a randomly coupled neuron network. Response  $Q$  of three randomly coupled neuron networks with different probability of connections vs the amplitude  $B$  of high-frequency driving: (a)  $p < 0.08$ ; (b)  $p > 0.08$ . The corresponding high-frequency driving amplitude  $B_{VR}$  vs the amount of neuron population: (c)  $p < 0.08$ ; (d)  $p > 0.08$ . The parameters are  $N=50$ ,  $f=50\%$ . This figure is the average result of ten trials.

linked to its  $K$  nearest neighbors, and replacing some links with new random ones with probability  $p$ . By increasing the probability  $p$  the architecture of the neuron population is tuned between the two extremes, regular and random networks. Small-world networks are characterized by low values of the probability  $p$ , as shown in Fig. 6.

The effect of the number of nearest neighbors on the VR in the neuron population is investigated first. In Fig. 7 three cases are reported:  $K=2$ ,  $K=4$ , and  $K=6$ . It is shown that the optimal amplitude of high-frequency driving  $B_{VR}$  will increase and the range of suitable high-frequency driving levels will reduce with the increase in  $K$ . It means that more local links will lead to more energy cost needed for VR in a small-world network of neuron population.

The effects of high-frequency driving in a small-world network of FHN have been characterized with respect to different values of the number of FHN units. The result is shown in Fig. 8(a), where it is evident that increasing the number of FHN units, the suitable high-frequency driving levels will be reduced. But the size of the neuron network has a little effect on the optimal amplitude of high-frequency driving, as shown in Fig. 8(b).

To increase the rewiring probability will introduce more long-range edges in the small-world network, but it only changes the suitable high-frequency driving levels and does not affect the optimal amplitude of high-frequency driving, as shown in Figs. 9(a) and 9(b), respectively.

### C. Mechanism of VR in different neuropopulations

In the absence of driving, Eqs. (3) and (4) can be cast in the form

$$\varepsilon \frac{dx_i}{dt} = x_i - \frac{x_i^3}{3} - y_i - I_i^{\text{syn}}, \quad (6)$$

$$\frac{dy_i}{dt} = x_i + a. \quad (7)$$

Then the so-called asymmetric double-well potential function<sup>1</sup> in the rest state of Eqs. (6) and (7) can be given as

$$V(x) = \frac{x^2}{2} - \frac{x^4}{12} - (a^3/3 - a + I^{\text{syn}})x. \quad (8)$$

The sketch of  $V(x)$  is shown in Fig. 10, from which we can see that  $V_{\text{th}}$ , the height of the potential barrier separating the two minima, determines the optimal strength of high-frequency driving of VR, and the synaptic current can change the value of  $V_{\text{th}}$  so as to affect VR in network with various topologies.

As the synaptic current can change the value of  $V_{\text{th}}$ , the optimal strength of high-frequency driving of VR is affected by the topology of network. For a random coupled network, the value of  $V_{\text{th}}$  will increase with the population of network, and if the connection probability is greater than a certain

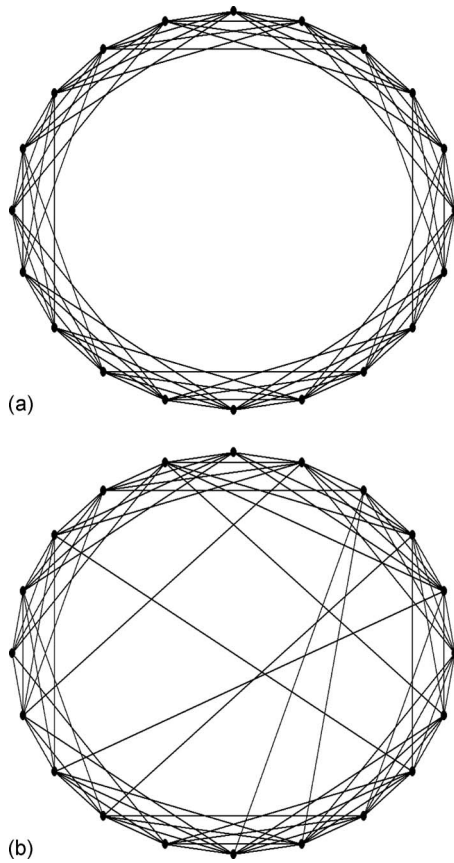


FIG. 6. Example of considered small-world network topologies. Given 20 isolated nodes. (a) Regular ring characterized by  $p=0$ . Each node is connected to its  $K=4$  nearest neighbors. (b) Realization of small-world topology via random rewiring of a certain fraction  $p=0.1$  of links.

threshold, the value of  $V_{th}$  will increase with the connection probability so the optimal strength of high-frequency driving of VR will increase the population of network and the connection probability. For a network with small-world properties, the value of  $V_{th}$  will not increase with the population of network and the reconnection probability, so we can obtain the results in Sec. III B.

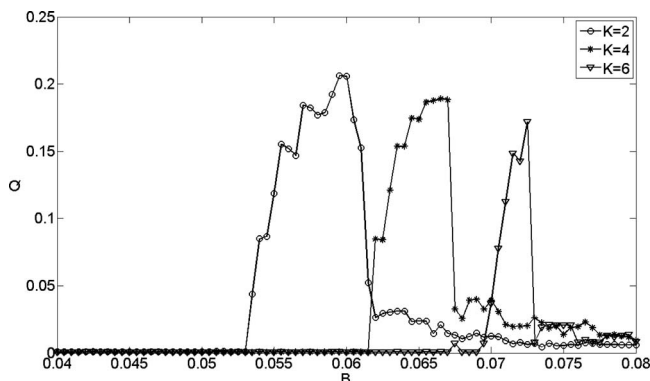


FIG. 7. Effect of the number of nearest neighbors on the VR in the neuron population of small-world network. The parameters are  $N=100$ ,  $p=0.1$ ,  $f=10\%$ . This figure is the average result of ten trials.

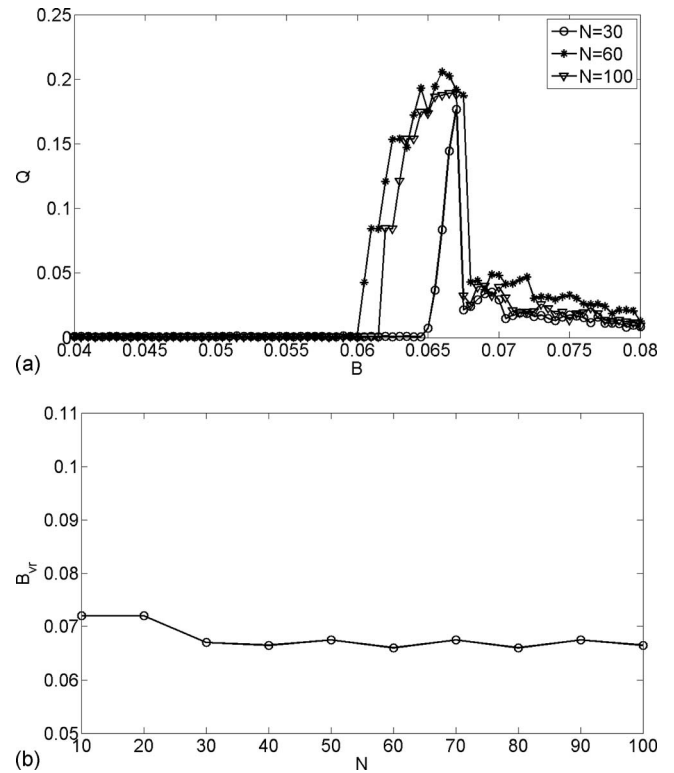


FIG. 8. Effect of the size of neuron network on the VR in a small-world neuron network. (a) Response  $Q$  of three small-world neuron networks with different amounts of elements vs the amplitude  $B$  of high-frequency driving. (b) The corresponding high-frequency driving amplitude  $B_{VR}$  vs the amount of neuron population. The parameters are  $K=4$ ,  $p=0.1$ ,  $f=10\%$ . This figure is the average result of ten trials.

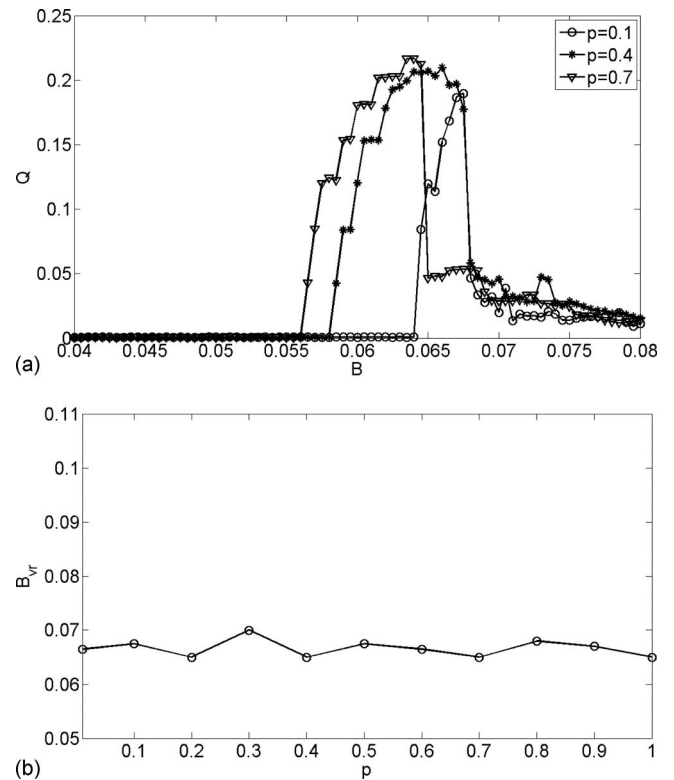


FIG. 9. Effect of the rewiring probability on the VR in a small-world neuron network. (a) Response  $Q$  of three small-world neuron networks with different rewiring probabilities vs the amplitude  $B$  of high-frequency driving. (b) The corresponding high-frequency driving amplitude  $B_{VR}$  vs rewiring probability. The parameters are  $K=4$ ,  $N=50$ ,  $f=10\%$ . This figure is the average result of ten trials.

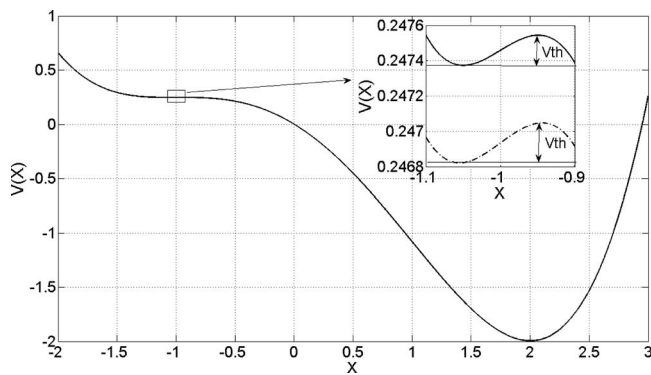


FIG. 10. Sketch of  $V(x)$ . The case in the absence of coupling (line) and the case which considers the effect of coupling (dashed line).

#### IV. CONCLUSIONS

In conclusion, we have studied the dynamical response of coupled neurons to bichromatic signal with two very different frequencies from the viewpoint of VR. Several topologies from random connected to small-world networks have been investigated. These systems behave in a very different way. For example, in the local input case, the larger the neuron population is, the more energy is needed for the emergence of VR in a randomly coupled neuron network, but the size of the small-world neuron network almost does not affect the optimal amplitude of high-frequency driving. It is because that although the connection will improve the performance of the system by increasing the information exchange among the neurons, the subthreshold oscillation of neurons will also transform among the network through electrical coupling, and the coupled neurons will respond to the input signal collectively only after the synchronization of subthreshold oscillation among the network. The ability to achieve synchronization in small-world network is much better than in random network, so the simulation results presented will be obtained. It is also noted that for a chain coupled neuron network the VR is enhanced evidently, and this is in accord with the results in Ref. 16.

We suspect that while almost every unit is connected the additional links will lead to more energy cost needed for VR in a neural network. So for a randomly coupled neuron population, if the connection probability is greater than a certain threshold, the optimal amplitude of high-frequency driving will increase with its increase, and for a small-world network, the optimal amplitude of high-frequency driving will

increase and the range of suitable high-frequency driving levels will reduce with the increase in the number of nearest neighbors. We also find that the addition of long-range edges in a small-world network only changes the suitable high-frequency driving levels and does not affect the optimal amplitude of high-frequency driving.

We expect our findings will be relevant for different fields in neuroscience including deep brain stimulation, where also high-frequency signal is used. Given the ubiquity of two-frequency signals in neuron assemblies and an optimal strength of high-frequency driving may enhance the transmission of information.

#### ACKNOWLEDGMENTS

This work is supported by the National Natural Science Foundation of China through Grant Nos. 50537030 and 50707020 and the Postdoctoral Science Foundation of China through Grant Nos. 20070410756 and 200801212.

- <sup>1</sup>L. Gammaitoni, P. Hänggi, P. Jung, and F. Marachesoni, *Rev. Mod. Phys.* **70**, 223 (1998).
- <sup>2</sup>D. Cubero, J. Casado-Pascual, J. Gómez-Ordóñez, J. Manuel Casado, and M. Morillo, *Phys. Rev. E* **75**, 062102 (2007).
- <sup>3</sup>C. Zhou, J. Kurths, and B. Hu, *Phys. Rev. E* **67**, 030101(R) (2003).
- <sup>4</sup>E. Ullner, dissertation, Institute of Physics, Potsdam University, 2004.
- <sup>5</sup>E. I. Volkov, E. Ullner, A. A. Zaikin, and J. Kurths, *Phys. Rev. E* **68**, 026214 (2003).
- <sup>6</sup>E. I. Volkov, E. Ullner, A. A. Zaikin, and J. Kurths, *Phys. Rev. E* **68**, 061112 (2003).
- <sup>7</sup>E. Ullner, A. Zaikin, J. García-Ojalvo, and J. Kurths, *Phys. Rev. Lett.* **91**, 180601 (2003).
- <sup>8</sup>E. Ullner, A. Zaikin, J. García-Ojalvo, R. Báscones, and J. Kurths, *Phys. Lett. A* **312**, 348 (2003).
- <sup>9</sup>V. N. Chizhevsky, *Int. J. Bifurcation Chaos Appl. Sci. Eng.* **18**, 1767 (2008).
- <sup>10</sup>V. N. Chizhevsky and G. Giacomelli, *Phys. Rev. A* **71**, 011801(R) (2005).
- <sup>11</sup>A. Zaikin, L. López, J. P. Baltanás, J. Kurths, and M. A. F. Sanjuán, *Phys. Rev. E* **66**, 011106 (2002).
- <sup>12</sup>G. M. Shepherd, *Foundations of the Neuron Doctrine* (Oxford University Press, New York, 1990).
- <sup>13</sup>M. Perc, *Phys. Rev. E* **76**, 066203 (2007).
- <sup>14</sup>S. H. Strogatz, *Nature (London)* **410**, 268 (2001).
- <sup>15</sup>J. F. Lindner, B. K. Meadows, W. L. Ditto, M. E. Inchiosa, and A. R. Bulsara, *Phys. Rev. Lett.* **75**, 3 (1995).
- <sup>16</sup>C. Zhou, J. Kurths, and B. Hu, *Phys. Rev. Lett.* **87**, 098101 (2001).
- <sup>17</sup>R. FitzHugh, *Biophys. J.* **1**, 445 (1961).
- <sup>18</sup>A. Pikovsky and J. Kurths, *Phys. Rev. Lett.* **78**, 775 (1997).
- <sup>19</sup>P. Glendinning, *Stability, Instability, and Chaos* (Cambridge University Press, Cambridge, 1994).
- <sup>20</sup>A. A. Zaikin, J. García-Ojalvo, L. Schimansky-Geier, and J. Kurths, *Phys. Rev. Lett.* **88**, 010601 (2001).
- <sup>21</sup>P. Erdős and A. Rényi, *Publ. Math. Inst. Hung. Acad. Sci.* **5**, 17 (1959).